Separation Science and Technology
Publication details, including instructions for authors and subscription information:
http://www.informaworld.com/smpp/title~content=t713708471

Supporting of Potassium Copper Hexacyanoferrate on Porous Activated Carbon Substrate for Cesium Separation

Li Wang[a]; Miao Feng[a]; Chunxia Liu[a]; Yongsheng Zhao[a]; Shuqiong Li[a]; Hang Wang[a]; Liang Yan[a]; Gan Tian[a]; Shoujian Li[a]
[a] College of Chemistry, Sichuan University, Chengdu, P. R. China

To cite this Article Wang, Li , Feng, Miao , Liu, Chunxia , Zhao, Yongsheng , Li, Shuqiong , Wang, Hang , Yan, Liang , Tian, Gan and Li, Shoujian(2009) 'Supporting of Potassium Copper Hexacyanoferrate on Porous Activated Carbon Substrate for Cesium Separation', Separation Science and Technology, 44: 16, 4023 — 4035

To link to this Article: DOI: 10.1080/01496390903183253

URL: http://dx.doi.org/10.1080/01496390903183253

Separation Science and Technology, 44: 4023–4035, 2009

ISSN: 0149-6395 print/1520-5754 online
DOI: 10.1080/01496390903183253

Supporting of Potassium Copper Hexacyanoferrate on Porous Activated Carbon Substrate for Cesium Separation

Li Wang, Miao Feng, Chunxia Liu, Yongsheng Zhao, Shuqiong Li, Hang Wang, Liang Yan, Gan Tian, and Shoujian Li
College of Chemistry, Sichuan University, Chengdu, P. R. China

Abstract: Activated carbon (AC) was chosen for carrying potassium copper hexacyanoferrate (KCuCF) to prepare a new Cs-selective material. The adsorbent was prepared by repetitious batch precipitation reaction of Cu^{2+} with $[Fe(CN)_6]^{4-}$. Characterization analyses identified the backbone formula of the activated carbon-supported KCuCF with $K_2Cu[Fe(CN)_6]$, and shown the successful loading of KCuCF microcrystals on the porous carbon substrate with a loading percentage of 12.5 wt%, and with BET specific surface area and a total pore volume of $527.8\,m^2/g$ and $0.38\,cm^3/g$ for AC and $160.8\,m^2/g$ and $0.16\,cm^3/g$ for KCuCF-loaded activated carbon (KCuCF-AC), respectively. The optimal Cs adsorption capacity of about $0.46\,mmol \cdot g^{-1}$ was observed between the HNO_3 concentration of 0.5–1.5 M, and the capacity even reached to $0.38\,mmol \cdot g^{-1}$ in the presence of a large amount of competing cations. The results indicate that activated carbon has no significant effect on the selectivity of the as-synthesized composite.

Keywords: Activated carbon, cesium, hexacyanoferrate, inorganic ion exchanger, separation

Received 3 February 2009; accepted 12 May 2009.

Address correspondence to Shoujian Li, College of Chemistry, Sichuan University, Chengdu 610064, P. R. China. Tel.: +86 28-85412329; Fax: +86 28-85412907. E-mail: sjli000616@163.com

INTRODUCTION

^{137}Cs is one of the most active components and a significant contributor to the heat in high-level radioactive liquid waste (HLLW) resulting from the reprocessing of spent fuel and other nuclear materials, due to its thermal output (0.07 W/g) and long half-life($T_{1/2} = 30$y). The removal of ^{137}Cs from HLLW not only would lower the radioactivity of HLLW and reduce storage problems, but also might achieve recovery of ^{137}Cs as an excellent source for gamma irradiators. Thus, the separation of ^{137}Cs from HLLW is significant for the treatment and disposal of nuclear wastes and the sustainable development of nuclear energy.

Over half a century, a wide variety of materials have been explored for the removal and/or separation of cesium. Among these materials, inorganic ion exchangers, such as zeolites (1–3), heteropolyacid salts, like ammonium molybdophosphate (AMP) (4), ammonium tungstophosphate (AWP) (5), etc., crystalline silicotitanates (CSTs)(6,7) and insoluble metal hexacyanoferrates (MHCFs) (8,9), have been broadly investigated, because of their better affinity towards cesium (10).

Previous studies demonstrated that MHCFs have strong selectivity for cesium over other radionuclides and alkali cations even in more acidic solutions (11,12). However, MHCFs prepared by mixing a solution of the transition metal salt with a solution of Hexacyanoferrates salt had small particle size and might even be colloidal, so the powder-like resultants were in fact unsuitable for practical application. In order to improve their mechanical properties, several investigators have resorted to the use of a support, and these include polyacrylonitrile binding polymer for CuHCF and NiHCF (13), porous silica for CuHCF (14) and NiHCF (15), zeolites for NiHCF (16,17), vermiculite for CuHCF (18). For a typical instance, Yue (19) reported the immobilization of copper ferrocyanide on mesoporous ceramic backbone. The fast-binding kinetics and high loading capacity have been achieved resulting from the rigidly open pore structure and extremely high surface area of the support. Further works performed by Yue (20) described the development of novel nanocomposite films by combining the high surface area of carbon nanotubes, the chemical stability of polyaniline, and the Cs ion exchange properties of NiHCF together, the material can remove radioactive cesium through an electrically switched ion exchange process.

Activated carbon (AC) is the most commonly used and effective porous adsorbent (21). Though exhibiting a poor binding affinity for interested radionuclides (such as ^{137}Cs and ^{90}Sr), activated carbon possesses a number of intrinsic advantages, including a well-developed pore structure, a large specific surface area, high thermal and mechanical stability, strong resistance to radiation damage, and especially, excellent endurance to extreme chemical environment compared with most of the inorganic and organic matrix. Besides, in view of the heat-releasing rate of 0.07 W/g · ^{137}Cs, the 773 K of kindling point of the coconut-shell AC used in this work, according to the technical index provided by manufacturers, would make more reliable safety for the Cs preconcentration by the AC-based adsorbent and subsequent ^{137}Cs extraction process, because ^{137}Cs would usually be recovered for extensive use as a radiation source and radioactive tracer before long-term storage. Taking the nature characters into account, we might have enough reason trying to make it as a promising support candidate for MHCFs. Furthermore, cesium-loaded MHCF-AC composite could be directly immobilized with mechanically strong and water-resistant matrices, like concrete and glass, and have a better compatibility with the final form in nuclear waste disposal process than other supports.

In this work, for the purpose of combining the inherent advantages of AC with the high Cs-selectivity and capability of KCuCF together, the synthesis and the characterization of KCuCF-AC composite was studied. Batch tests were also performed to evaluate the Cs-adsorbing properties of the new adsorbent.

EXPERIMENTAL SECTION

Preparation of KCuCF-AC

Coconut shell activated carbon (0.35~0.45 mm) was treated with HNO_3 (14 M) for 24 h at room temperature, washed with several aliquots de-ionized water till ca. pH = 5.0 and then ethanol, followed by being air-dried at 363 K for 3 h.

The pretreated activated carbon (1 g) was impregnated with 10 cm^3 solution of $CuSO_4$ (0.5 M) under vacuum condition for 4 h. The supernate was decanted, and 5 cm^3 solution of $K_4[Fe(CN)_6]$ (0.5 M) was added drop-wise under agitation at room temperature. The obtained reddish-brown slurries were aged at 353 K for 12 h, then washed with de-ionized water, filtered using a Buchner funnel with suction, followed by being dried in the air at 373 K for 4 h. Density-difference separation was employed in this stage to remove the fine particles of KCuCF that had not clung or embedded on the internal and external surface of AC. The resulting products were prepared by repeating the forementioned procedure three times. The loading percentage attained to 12.5 wt% base on weight gain.

Characterization of KCuCF-AC

Infrared absorption spectra (FTIR) were measured with Perkin-Elmer IR-843 spectrometer by diluting solid samples in KBr and pressed into sheet form. Powder X-ray diffraction patterns were recorded by DX-1000 CSC X-ray diffractometer with a Cu Kα radiation (40 kV, 25 mA). The surface morphology and chemical components of the samples were characterized by scanning electron microscope Philips XL-3 (SEM, FEI Company, Oregon, USA) associated with energy dispersive spectroscopy (EDS, INCA PentaFET × 3, Oxford UK). Samples were mounted on suitable substrates using conductive glue and were then coated with a thin layer of gold. Nitrogen adsorption isotherms and pore properties of the materials were determined at 77 K using nitrogen on an auto ZXF-06 Porosity Analyzer.

Adsorption Experiments

Fractions (typically ca. 20 mg) of KCuCF-AC was dispersed in 20 cm^3 CsCl solution (2×10^{-3} M) with desired nitric acid concentration. The mixture was shaken (~175 rpm) for the specified time at room temperature. After the separation of the solid phase from the liquid, a portion of the filtrate was taken for cesium measurement. The concentration of Cs^+ was measured using a flame atomic adsorption spectroscopy (AAS), other metal elements, if presents, in the solution were analyzed by inductively coupled plasma atomic emission spectroscopy (ICP/AES).

Ion distribution coefficients (K_d, $dm^3 \cdot g^{-1}$) and cesium capacity (Q, $mmol \cdot g^{-1}$) were calculated by the equations below, respectively.

$$K_d = \frac{(C_0 - C_e)/M}{C_e/V} \qquad Q = \frac{(C_0 - C_e) \times V}{M}$$

Where C_e is the equilibrium concentration of metal ion ($mmol \cdot dm^{-3}$), C_0 is the initial concentration ($mmol \cdot dm^{-3}$), V is the volume of the testing solution (dm^3), and M is the amount of adsorbents (g).

RESULTS AND DISCUSSION

Characterization of the Composite

Infrared spectrum. Infrared spectroscopy was used to check the cyano group in KCuCF. The FTIR spectra of AC and KCuCF-AC composites are shown in Fig. 1. The plot of KCuCF-AC is similar to that of AC, except the sharp and strong peak at 2079 cm^{-1} corresponding to the $C{\equiv}N$ stretching vibration, which offers the evidence that KCuCF is loaded on the AC, after carefully isolated from the mentioned preparing system.

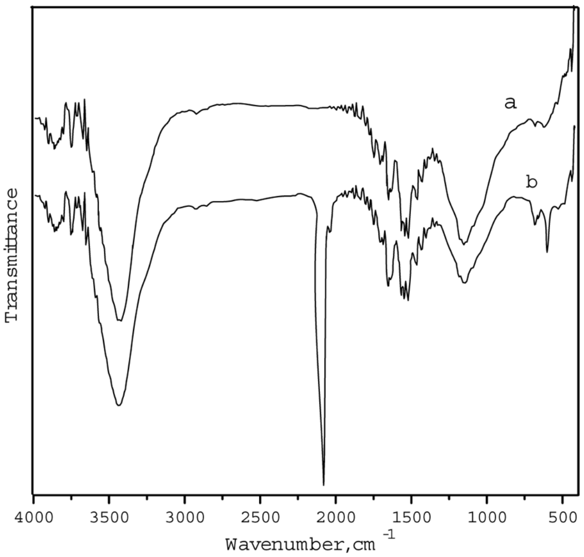

Figure 1. Infrared spectra of activated carbon (a) and KCuCF-AC composite (b).

X-ray analysis. The X-ray powder diffraction pattern of the carbon supported KCuCF is shown in Fig. 2a. The positions of the main diffraction peaks of the composite, e.g., 18.02° (200), 24.78° (202),

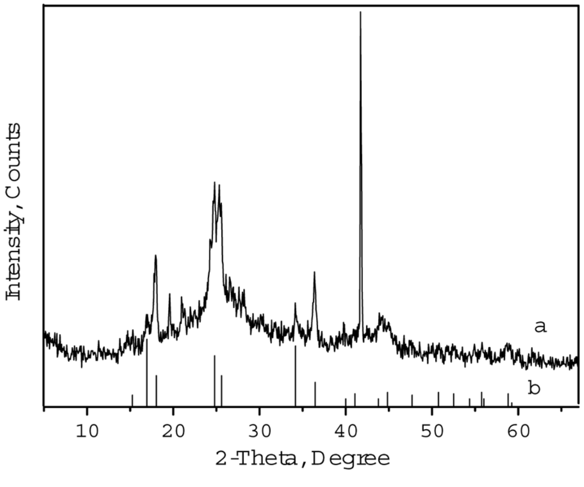

Figure 2. XRD powder patterns of KCuCF-AC composite (a) and K_2Cu $[Fe\ (CN)_6]$ (b).

25.58°(220), 34.16° (004), 36.42°(400), correspond well to those of $K_2Cu[Fe(CN)_6]$ (JCPDS Card No. 20-0875) shown in Fig. 2b. And the sharp peaks in Fig. 2a also suggest the crystalline state of KCuCF for the tested sample.

SEM-EDS studies. The microstructure images from surfaces of AC and KCuCF-AC observed by SEM (Figs. 3a, 3b respectively) exhibit a clear porous surface structure of both the samples. The fine KCuCF crystals are seen to be precipitated onto the internal/external surfaces of the 3D framework of the activated carbon.

The EDS spectrum pattern from Fig. 3c shows the strong carbon peak from the AC matrix. Besides the K, Cu, and Fe peaks from the KCuCF crystalloid supported on the surface of AC are also observed. However, after KCuCF-AC was contacted with the solution containing Cs^+ for 24 h, the K peak on the spectrum in Fig. 3c disappeared and was almost completely replaced by Cs band in Fig. 3d. The result indicates that Cs has been incorporated into the AC-carried KCuCF referring to an ion exchange process with K^+. Based on the data from EDS analysis, the empirical composition of

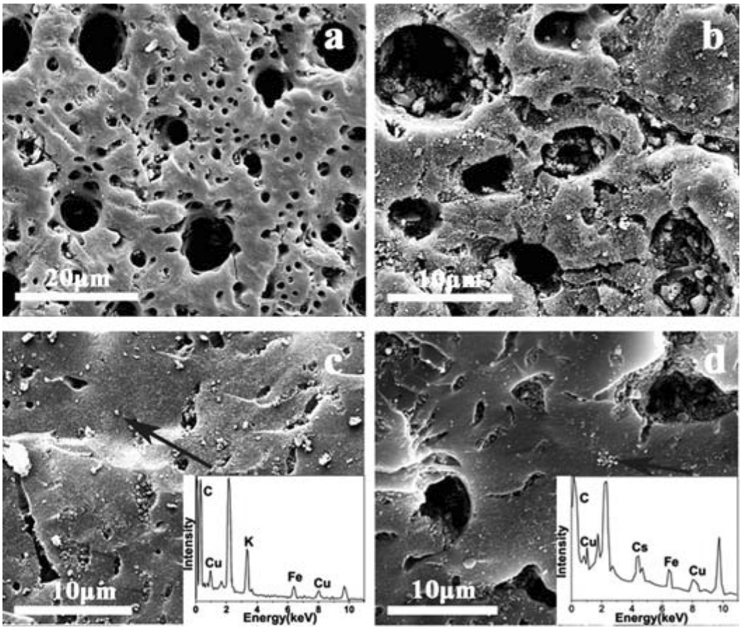

Figure 3. SEM patterns of activated carbon (a) and KCuCF-AC composite (b); EDX area analysis of KCuCF-AC (c) and Cs-loaded KCuCF-AC (d).

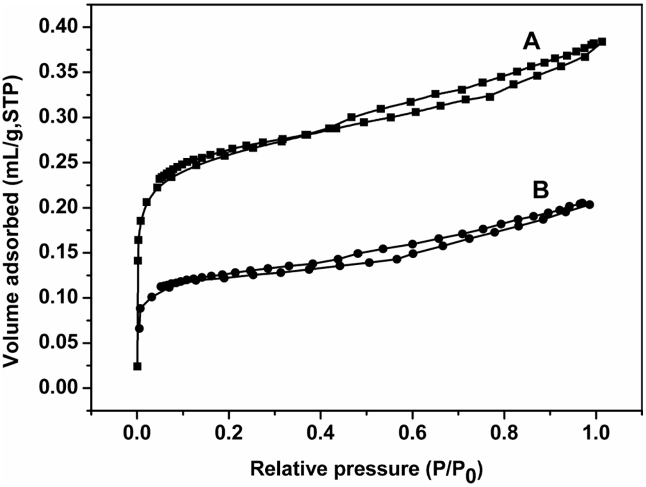

Figure 4. Adsorption/desorption isotherm of nitrogen, at 77 K, on AC (A) and KCuCF-AC composites (B).

KCuCF on the AC surface might suppose to be $K_{1.78}Cu_{1.25}Fe(CN)_6$, which basically accords with the result from the powder XRD for the as-prepared adsorbent.

Pore structure analysis. As shown by the nitrogen adsorption isotherms (Fig. 4) and related experimental data (Table 1), the BET specific surface areas and total pore volume reduced from 527.8 m^2/g and 0.38 cm^3/g for AC to 160.8 m^2/g and 0.16 cm^3/g for KCuCF-AC, respectively. The results suggest that the pores of AC were considerably blocked by loading of KCuCF microcrystals. On the other hand, the average pore diameter and the proportion of the mesopore diameter increased after loading KCuCF, which indicates that the microcrystal of KCuCF mainly blocked the micropore of the support.

Table 1. Pore characteristics of AC and KCuCF-AC samples

				Proportion of pore diameter (%)	
Sample	S_{BET}(m^2/g)	Vs (cm^3/g)	R mean (nm)	Micropore	Mesopore
AC	527.8	0.38	1.65	22.05	76.89
KCuCF-AC	160.8	0.16	2.09	10.84	88.32

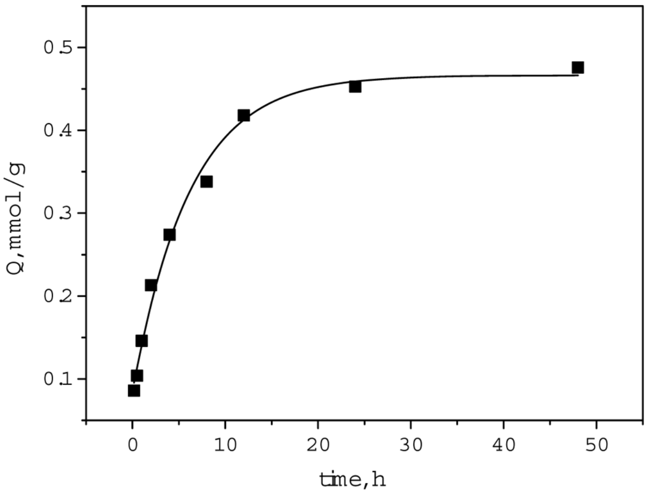

Figure 5. Effect of contact time on cesium adsorption capacity.

Effect of Contact Time

As shown in Fig. 5, the adsorption capacity of Cs^+ increased rapidly with the increase of contact time till 12 h, and then the increasing rate slowed down gradually. No significant enhancement is observed for the Cs adsorption in the duration of 24 h ~ 48 h. This suggests a slow ion exchange process between Cs^+ in solution and K^+ in KCuCF microcrystals impregnated on the support. Different with the fast monolayer adsorption of Cs onto the CuHCF-EDA-SAMMS interface (19), sufficient time would be necessary for Cs^+ ions to diffuse from the solution into the microcrystal for exchanging with K^+. The optimal shaking time was set at 24 h for succeeding experiments based on the results, except those described otherwise.

Effect of Nitric Acid Concentration

Figure 6 shows the cesium capacity of KCuCF-AC in solutions of varying nitric acid concentration. In low acidity range, the capacity is observed to increase steeply with acid concentration to a plateau when the concentration of HNO_3 close to 0.5 M, and then decrease gradually after 1.5 M. The results indicate that the as-prepared composite has the optimal adsorption capability (ca. $0.46\,mmol \cdot g^{-1}$) for Cs^+ between 0.5–1.5 M of HNO_3. Furthermore, the capacity keeps higher than

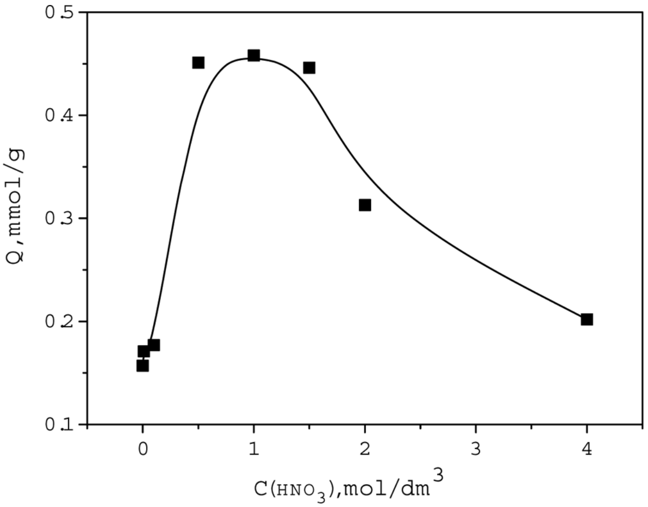

Figure 6. Effect of solution acidity on cesium adsorption capacity.

$0.3\,\mathrm{mmol \cdot g^{-1}}$ even at higher acidity of 2 M. Actually, the Cs capacity of pure KCuCF according to 12.5 wt% of the as-synthesized composite reaches to 3.68 mmol/g, a little higher than 3.19 mmol/g of CuFCN in ref. 11.

Effect of Competing Cations

The effect of the coexisting mono-, di-, and trivalent cations on Q and K_d was determined in 0.5 M of HNO_3 medium to investigate the Cs-selectivity of the as-prepared composite. The experimental data were

Table 2. Distribution behavior of cesium and competing cations on activated carbon and KCuCF- AC[a]

	Cs^+	Sr^{2+}	Ni^{2+}	Na^+	Fe^{3+}	Co^{2+}
$K_{d,\ \mathrm{KCuCF\text{-}AC}}$, dm · g	178.84	5.44	0.24	29.43	4.47	12.97
$K_{d,\ \mathrm{AC}}$, $\mathrm{dm^3 \cdot g^{-1}}$	10.91	10.94	6.09	94.26	30.16	1.18
$Q_{\mathrm{KCuCF\text{-}AC}}$, $\mathrm{mmol \cdot g^{-1}}$	0.38	0.009	0.001	0.064	0.004	0.011
Q_{AC}, $\mathrm{mmol \cdot g^{-1}}$	0.023	0.018	0.025	0.14	0.027	0.001

[a] Initial concentration of tested ions is 2×10^{-3} M for Cs^+, 2×10^{-3} M for Sr, 4×10^{-3} M for Ni, 0.01 M for Na, 4×10^{-3} M for Fe, 4×10^{-3} M for Co, respectively.

Table 3. Summary of various MHCFs materials adsorption behaviors for Cs^+

MHCFs	Carrier	Acidity	Q_{max} (mmol/g)	$C_{i,\ Cs+}{}^*$ (M)	Contact time	Ref. no.
KCoFC	–	$pH = 2.0 \sim 6.5$	1.72	0.01	3 days	12
CuFCN	–	0.5 $MHNO_3$	3.19	4×10^{-3}	4 hours	11
CuHCF	EDASAMMS	0.1 MHNO3	1.33	1.7×10^{-3}	2 hours	19
NiHCF	PEDTAFS	–	1.69	4.5×10^{-3}	–	15
KNiFC	Clinoptilolite	–	–	1.5×10^{-3}	24 hours	17
KNiFC	Chabazite	$pH = 3.70 \sim 5.83$	1.87	$10^{-2} \sim 0.1$	2 days	16
CoHCF	Graphite	$pH = 1 \sim 11$	–	$10^{-5} \sim 0.01$	Electrochemically control	22
NiHCF	Carbon nanotube	–	–	–	Electrochemically control	20
KCuFC	AC	0.5–1.5 MHNO3	0.48	2×10^{-3}	24 hours	present work

$^*C_{i,\ Cs^-}$–initial concentration of Cs^+.

summarized in Table 2. It can be seen that the total loading capacity for all cations in the system appear to be $0.47\,\text{mmol}\cdot\text{g}^{-1}$ while the cesium capacity is still up to $0.38\,\text{mmol}\cdot\text{g}^{-1}$ (80.9% of the total capacity), just slightly down from $0.46\,\text{mmol}\cdot\text{g}^{-1}$ for Cs^+ obtained in the absence of competitive cations. And the selectivity sequence of the adsorbent for all existing ions can be provided from the data in Table 2 as $Cs \gg Na > Co > Sr > Fe > Ni$. The KCuCF-AC composite exhibits extra high Cs^+ preferential affinity, even when concentrations of competitive cations being several times higher than that of cesium. The results suggest that the as-synthesized product still keeps the excellent feature of the hexacyanoferrate for the mutual separating of Cs^+ from other cations tested here.

Finally, related data characterizing the Cs adsorption behaviors for the as-synthesized adsorbent and different MHCFs materials reported previously are listed in Table 3. It could be understood that the adsorption behaviors of Cs ion on insoluble hexacyanoferrates strongly depends on the composition and structure types of the MHCFs, the preparing method, and the supports used. The differences lead to different physical- and chemical properties and adsorption behaviors of various MHCFs materials (22–24).

CONCLUSION

KCuCF particulates were loaded on the porous matrix of granular coconut-shell activated carbon by repeating the controlled batch precipitation reaction of $CuSO_4$ with K_4 [Fe $(CN)_6$]. The resulting KCuCF-AC composite shows a high selectivity and adsorption capacity for cesium in high salt and acidic solution. EDS analyses for the materials before and after adsorption reveals that Cs^+ in solution have been incorporated into the composite which may refer to an ion exchange process with K^+ on the solid KCuCF. The combination of intrinsic advantages of both activated carbon and potassium copper hexacyanoferrate(II) makes KCuCF-AC composite a strong candidate for the removal of cesium from acidic nuclear wastewater and endows it with an excellent compatibility with the various matrices employed in the solidification of nuclear wastes.

ACKNOWLEDGMENTS

The financial support from the National Natural Science Foundation of China (Grant 20571053 and 20871086) is gratefully acknowledged.

REFERENCES

1. Sinha, P.K.; Panicker, P.K.; Amalraj, R.V. (1995) Treatment of radioactive liquid waste containing cesium by indigenously available synthetic zeolites: A comparative study. *Waste Manage.*, *15* (2): 149–157.
2. Dyer, A.; Aggarwal, S. (1997) Removal of fission products from mixed solvents using zeolites. Part 2. Cesium and strontium removal. *J. Radioanal. Nucl. Chem.*, *221* (1–2): 235–238.
3. Mon, J.; Deng, Y.J.; Flury, M.; Harsh, J.B. (2005) Cesium incorporation and diffusion in cancrinite, sodalite, zeolite, and allophone. *Microporous Mesoporous Mater.*, *86* (1–3): 277–286.
4. Murthy, G.S.; Reddy, V.N.; Satyanara, J. (1997) Isolation of cesium from fission product waste solution on a new granular inorganic exchanger titanium phosphate-ammonium phosphomolybdate (TiP- AMP). *Special Publication – Royal Society of Chemistry*, *196* (Progress in Ion Exchange): 289–297.
5. Mimura, H.; Saito, M.; Akiba, K.; Onodera, Y. (2000) Selective uptake of cesium by ammonium tungstophosphate (AWP)-calcium alginate composites. *Solvent Extr. Ion. Exch.*, *18* (5): 1015–1027.
6. Anthony, R.G.; Dosch, R.G.; Gu, D. (1994) Use of silicotitanates for removing cesium and strontium from defense waste. *Ind. Eng. Chem. Res.*, *33* (11): 2702–2705.
7. Celestian, A.J.; Kubicki, J.D.; Hanson, J. (2008) The mechanism responsible for extraordinary Cs ion selectivity in crystalline silicotitanate. *J. Am. Chem. Soc.*, *130* (35): 11689–11694.
8. Sun, K.S.; Teng, H.C.; Chen, C.L. (2001) Preparation of the hexacyanoferrate ion exchangers and performance tests of the exchangers for removing cesium nuclide from radioactive wastewaters. *Nuclear Science Journal*, *38* (1): 46–58.
9. Harjula, R.; Lehto, J.; Paajanen, A. (2001) Removal of radioactive cesium from nuclear waste solutions with the transition metal hexacyanoferrate ion exchanger CsTreat. *Nucl. Sci. Eng.*, *137* (2): 206–214.
10. Gaur, S. (1996) Determination of Cs-137 in environmental water by ion-exchange chromatography. *J. Chromatogr. A*, *733* (1–2): 57–71.
11. Wang, Q.P.; Song, C.L.; Jiang, C.Y. (2000) Sieving of inorganic ion exchangers. *Ion Exchange and Adsorption*, *16* (3): 225–233.
12. Moon, J.K.; Lee, E.H.; Kim, H.T. (2004) Ion exchange of Cs ion in acid solution with potassium cobalt hexacyanoferrate. *Korean J. Chem. Eng.*, *21* (5): 1026–1031.
13. Someda, H.H.; Zahhar, A.A.; Shehata, M.K. (2002) Supporting of some ferrocyanides on polyacrylonitrile (PAN) binding polymer and their application for cesium treatment. *Sep. Purif. Technol.*, *29* (1): 53–61.
14. Milonji, S.; Bispo, I.; Fedoroff, M.; Loos, N.C. (2002) Sorption of cesium on copper hexacyanoferrate/polymer/silica composites in batch and dynamic conditions. *J. Radioanal. Nucl. Chem.*, *252* (3): 497–501.
15. Chang, C.Y.; Chau, L.K.; Hu, W.P. (2008) Nickel hexacyanoferrate multilayers on functionalized mesoporous silica supports for selective sorption and sensing of cesium. *Microporous Mesoporous Mater.*, *109* (1–3): 505–512.

16. Mimura, H.; Kimura, M.; Akiba, K. (1999) Selective removal of cesium from sodium nitrate solutions by potassium nickel hexacyanoferrate-loaded chabazites. *Sep. Sci. Technol.*, *34* (1): 17–28.
17. Kazemian, H.; Zakeri, H.; Rabbani, M.S. (2006) Cs and Sr removal from solution using potassium nickel hexacyanoferrate impregnated zeolites. *J. Radioanal. Nucl. Chem.*, *268* (2): 231–236.
18. Huang, C.T.; Wu, G. (1999) Improvement of Cs leaching resistance of solidified radwastes with copper ferrocyanide (CFC)-vermiculite. *Waste Manage.*, *19* (4): 263–268.
19. Lin, Y.H.; Fryxell, G.E.; Wu, H. (2001) Selective sorption of cesium using self-assembled monolayers on mesoporous supports. *Environ. Sci. Technol.*, *35* (19): 3962–3966.
20. Lin, Y.H.; Cui, X.L. (2005) Novel hybrid materials with high stability for electrically switched ion exchange: Carbon nanotube–polyaniline–nickel hexacyanoferrate nanocomposites. *Chem. Commun.*, *17*: 2226–2228.
21. Hristovski, K.D.; Westerhoff, P.K.; Crittenden, J.C. (2008) Arsenate removal by iron (Hydr) oxide modified granulated activated carbon: Modeling arsenate breakthrough with the pore surface diffusion model. *Sep. Sci. Technol.*, *43* (11 & 12): 3154–3167.
22. Green-Pedersen, H.; Korshin, G.V. (1999) Separation of cesium from high ionic strength solutions using a cobalt hexacyanoferrate-modified graphite electrode. *Environ. Sci. Technol.*, *33* (15): 2633–2637.
23. Ayrault, S.; Jimenez, B,; Garnier, E. (1998) Sorption mechanisms of cesium on (Cu2FeII)-Fe-II(CN)(6) and Cu-3(II)[Fe-III(CN)(6)](2): Hexacyanoferrates and their relation to the crystalline structure. *J. Solid State Chem.*, *141* (2): 475–485.
24. Loos-Neskovic, C.; Ayrault, S.; Badillo, V. (2004) Structure of copper-potassium hexacyanoferrate (II) and sorption mechanisms of cesium. *J. Solid State Chem.*, *177* (6): 1817–1828.